The Bioscan
AN INTERNATIONAL QUARTERLY JOURNAL OF LIFE SCIENCES
20(4): 1289-1307, 2025 www.thebioscan.com

Computational Investigation of SomeXanthene-Based Molecules for Optoelectronic Properties: DFT and TD-DFT Study

Saravana Priya Esakki Durai[1], Sumitha Selvanayakam[2] and Swarnalatha Kalaiyar[3*]

[1]Research Scholar, Photochemistry Research Laboratory, Department of Chemistry, Manonmaniam Sundaranar University, Abishekapatti, Tirunelveli – 627 012, Tamil Nadu, India.
E-mail id: priyasan21riya@gmail.com ; ORCID ID: 0000-0002-5136-7190
[2]Research Scholar, Photochemistry Research Laboratory, Department of Chemistry, Manonmaniam Sundaranar University, Abishekapatti, Tirunelveli – 627 012, Tamil Nadu, India.
E-mail id: anisumitha@gmail.com
[3]Professor, Photochemistry Research Laboratory, Department of Chemistry, ManonmaniamSundaranar University, Abishekapatti, Tirunelveli – 627 012, Tamil Nadu, India
E-mail id: swarnalatha@msuniv.ac.in; ORCID ID: 0000-0002-8009-6924

***Corresponding Author:** Dr. Swarnalatha Kalaiyar, E-mail id: swarnalatha@msuniv.ac.in

DOI: 10.63001/tbs.2025.v20.i04.pp1289-1307

KEYWORDS
Optoelectronic properties; Xanthene; DFT; light-emitting; excitation energy.

Received on:

15-09-2025

Accepted on:

18-11-2025

Published on:

16-12-2025

ABSTRACT

In this study, we present the design and theoretical investigation of four xanthene-based molecules such as fluorescein (F), fluorescein hydrazide (FH), 2-((4-(dimethylamino) benzylidene) amino)-3′,6′- dihydroxyspiro[isoindoline-1,9′-xanthen] 3-one (DMAB-HIX) and 2-((anthracen-9-ylmethylene) amino)-3',6'-dihydroxyspiro[isoindoline-1,9'-xanthen]-3-one (ANT-HIX) to explore the optical and electronic properties for potential application in optoelectronic devices. Density functional theory (DFT) and time-dependent density functional theory (TD-DFT) calculations were employed to evaluate frontier molecular orbitals, chemical reactivity descriptors, absorption and emission spectra, excitation binding energies, excited-state lifetime and light-harvesting efficiencies. The results reveal that molecular functionalization significantly influences the optoelectronic behaviour of the studied systems. In particular, DMAB-HIX shows a shorter excited-state lifetime, higher light-harvesting efficiency and a lower HOMO-LUMO energy gap, attributed to the strong electron-donating effect of the dimethylamino substituents (DMA). These finding establish clear structure-property relationships and suggest that DMAB-HIX shows potential as a high-performance OLED emissive material.

1. Introduction

In recent years, organic materials have attracted considerable interest due to their potential applications across diverse fields, including electronic devices, capacitors, hybrid films, photosensitizers, metal-organic frameworks, metal sensing in biological organisms, drug delivery systems and various biomedical applications[1]. Electronic devices play a pivotal role in modern technology by efficiently converting electrical energy into light, thereby

supporting the global shift towards sustainable and energy-efficient systems. As the demand for flexible and sustainable optoelectronic devices continues to rise, the exploration of innovative and optimized light-emitting materials has become crucial for advancing technology[2,3]. Recently, a range of light-emitting materials has emerged, including polymer-based materials, nanomaterials and organic compounds[4]. Organic molecule-based optoelectronics have gained popularity due to their numerous advantages, such as high flexibility, straightforward design processes, low fabrication costs, easy processing and the possibility of large-scale production[5,6]. In particular, organic materials have been extensively utilized in display technology, finding applications in OLEDs, micro-OLEDs, LCDs, lasers and photodiodes through thin film methods and solution processing techniques[7,8]. One of the biggest challenges in organic electronics is the development of organic optoelectronic materials with desirable photophysical properties, which is essential for applications like organic light-emitting diodes, organic photovoltaics and organic field-effect transistors[9]. The performance of these organic electronics devices hinges on the composition of the active layers, application methods and processing conditions. Typically, the active layers comprise donor-π-acceptor structures featuring various aromatic π-conjugated small molecules or polymers, including triphenyl amine[10], thiophene[11], carbazole[12], imidazole[13] and anthracene[14].

This study presents a theoretical analysis of the optical and electronic properties of four xanthene-based organic molecules, which are promising candidates for green OLEDs. The ground and first excited state geometries of these molecules were fully optimized. Utilizing the optimized structure, we calculated the frontier molecular orbitals, total electron density, density of state and Mulliken atomic charges. Furthermore, we evaluated the electronic transition energy, oscillator strength and maximum electron contribution orbitals. subsequently, a time dependent density functional theory(TD-DFT) approach was employed to simulate the optical absorption and emission spectra of these molecules[15]. From the absorption study results, alongside the calculated oscillator strength and electron transition energy, we assessed the excited state life time and light-harvesting efficiency of the molecules. Based on these properties, the light emitting capacity of the molecules were studied.

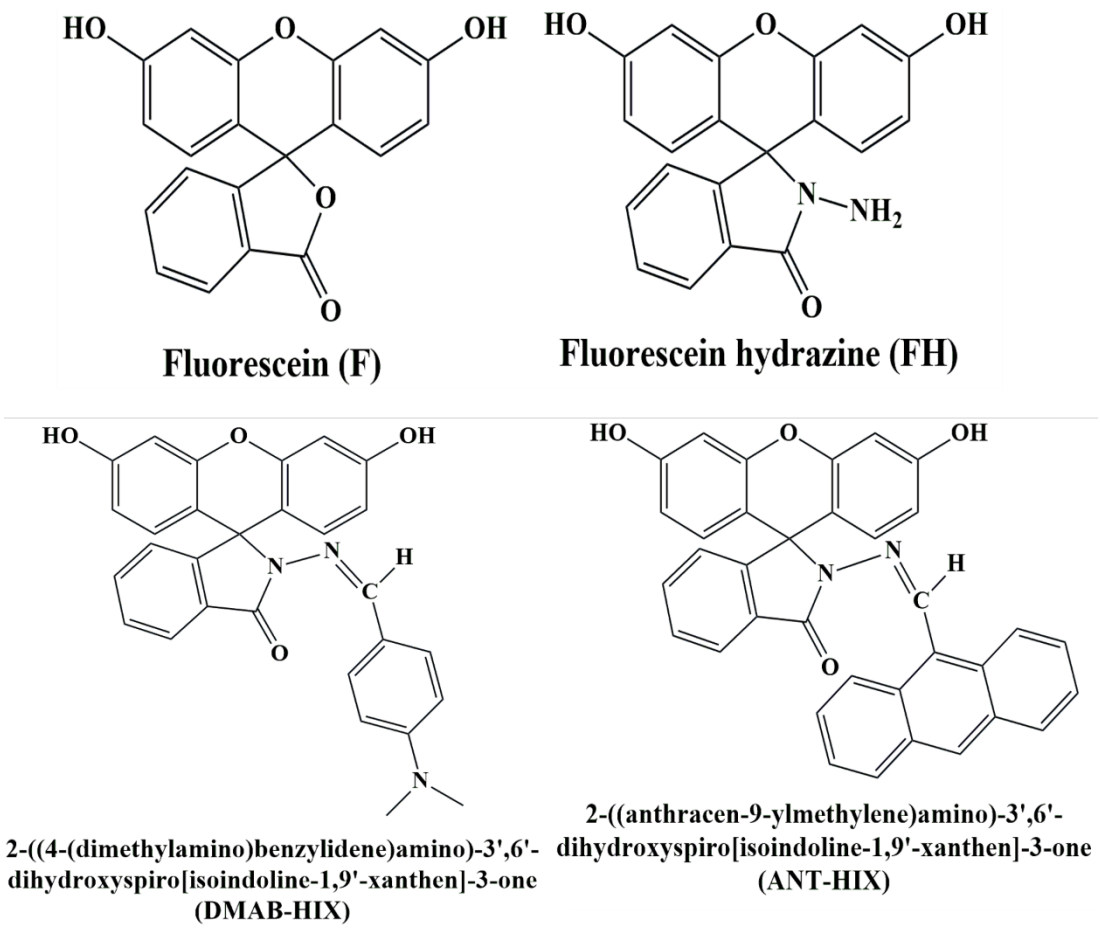

Fig. 1 Structure of functionalized xanthene molecules

2. Results and discussion

2.1 Molecular geometry

Three fluorescein-derived molecules were designed and examined using density functional theory (DFT). The two-dimensional structure of the designed molecules was shown in Fig. 1. First, the parent fluorescein (F) structure was optimized, followed by its hydrazine-modified derivative (FH). Subsequently, two additional derivatives: FH functionalized with N,N-dimethylaminobenzyl (DMAB-HIX) and FH functionalized with anthracene methylene (ANT-HIX) were optimized at the DFT/B3YLP 6-31G (d,p) level of theory. The optimized structure was depicted in Fig. 2. The results show that the xanthene moiety retains a predominantly planar conformation, whereas th attached spirolactam ring is oriented nearly perpendicular to the xanthene plane. Overall, all four functionalized xanthene-based molecules exhibit non-planar geometries due to the torsional arrangement introduced by the spirolactam and substituent groups.

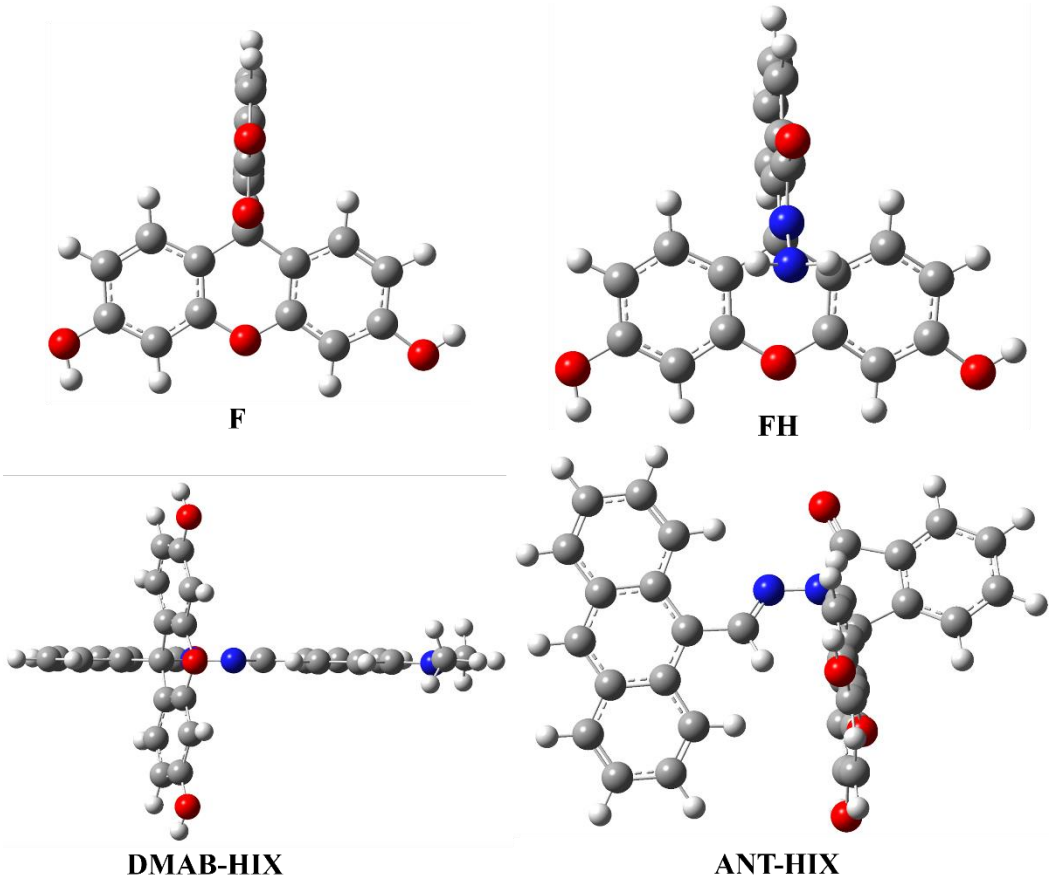

Fig. 2 Optimized structures of studied molecules

2.2

Electronic properties

The investigation of optoelectronic behavior and charge transfer characteristics in conjugated molecules necessitated an in-depth examination of the energy levels of the highest occupied molecular orbital (HOMO) and the lowest unoccupied molecular orbital (LUMO). These energy parameters were critical for evaluating the charge-transfer efficiency between donor and acceptor groups within the studied molecules[16]. In this work, the electronic structures were calculated using the DFT/B3LYP/6-31G(d,p) computational method, which enabled precise determination of the HOMO and LUMO energy levels. The energy gap (E_{gap}) was defined as the difference between these two energy levels.

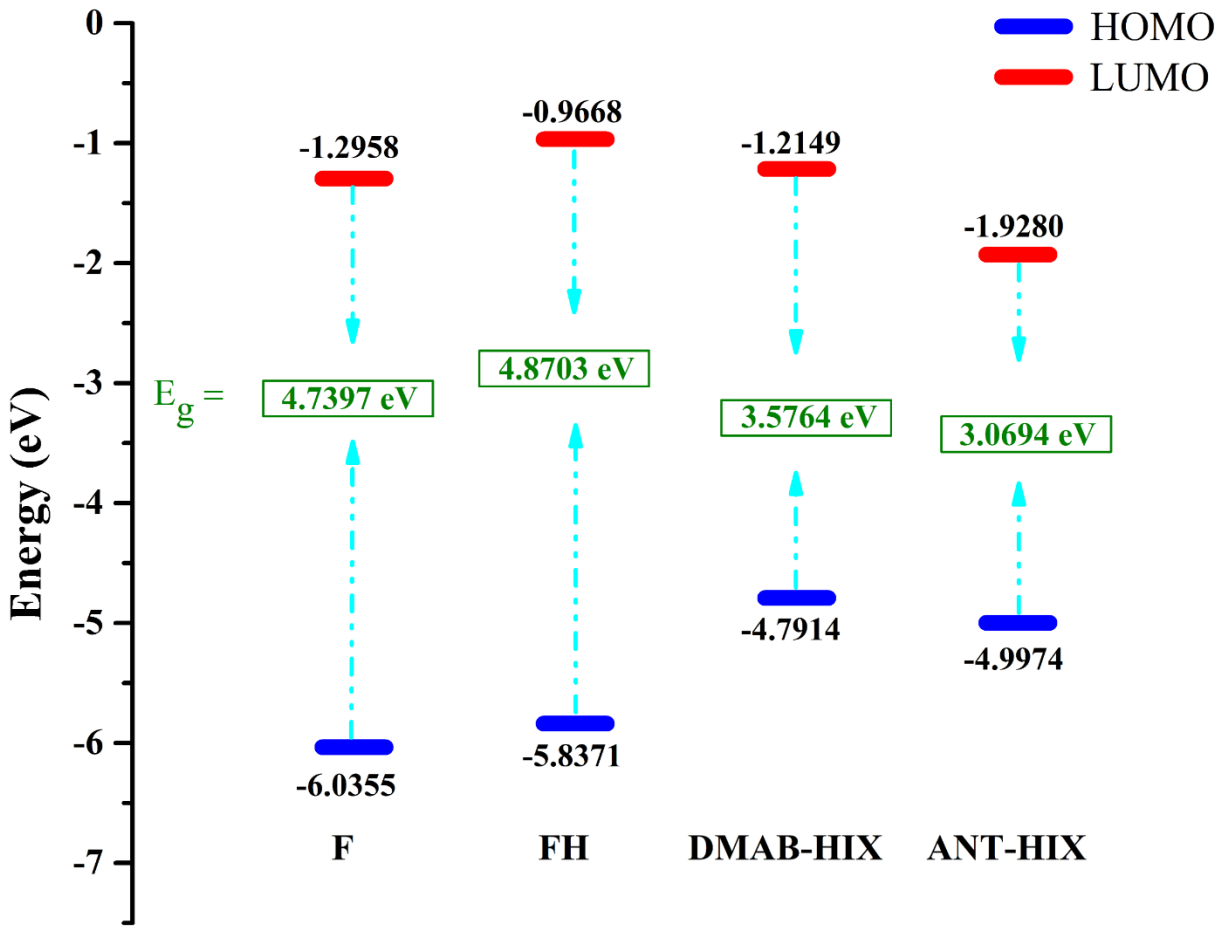

Fig. 3 Electronic structure of studied molecules

According to the results, the electron-denoting ability (based on HOMO energy levels) followed the order: DMAB-HIX (-4.7964 eV) > ANT-HIX (-4.9974 eV > FH (-5.8371 eV) > F (-6.0355 Ev). Similarly, the electron-withdrawing tendency (based on LUMO energy levels) decreased in the sequence: FH (-0.9668 eV) > DMAB-HIX (-1.2149 eV) > F (-1.2958 eV) > ANT-HIX (-1.9280 eV). The calculated E_{gap}values exhibited notable variation among the molecules, increasing in following order: 3.0694 eV < 3.5764 eV < 4.7397 eV <4.8703 eV. Fig. 3 presents the theoretical values of E_{HOMO}, E_{LUMO} and E_{gap}. Among the four molecules, FH displayed the widest HOMO-LUMO separation (4.8703 eV), indicating relatively lower charge-transfer efficiency. In the DMAB-HIX molecule, the reduced energy gap can be attributed to the presence of strong electron-donating N.N-dimethyl amino (DMA) groups. The nitrogen atom in DMA enhanced local electron density through its lone-pair contribution, leading to a redistribution of electronic charge that

effectively narrowed the HOMO-LUMO gap. In contrast, ANT-HIX which lacks a strong electron donation group, exhibited a slightly diminished energy gap relative to DMAB-HIX due to its extended π-conjugation and planar anthracene ring system. This structural planarity enhanced electron delocalization, exerting a synergistic effect on conjugation. A smaller HOMO-LUMO energy gap implies that electronic excitation from the HOMO to the LUMO can occur with lower photon energy, corresponding to absorption at longer wavelengths. Therefore, the relatively narrow energy gaps of DMAB-HIX and ANT-HIX suggest their suitability for optoelectronic applications, where efficient light absorption and emission at extended wavelengths are desirable.

2.3 Molecular electrostatics potential

Molecular electrostatic potential provides a visual representation of the charge distribution within a molecule and serves as an effective tool for understanding its relative polarity. It is directly related to the electronic density and acts as a valuable descriptor for identifying the reactive sites of a molecule. To predict the probable sites for electrophilic and nucleophilic attacks, the MEP of the compound was computed at the optimized molecular geometry and is depicted in fig.4. In the MEP map, different electrostatic potential values are depicted using a colour scale, typically represented by red, green and blue regions, corresponding to areas of negative, neutral and positive electrostatic potential, respectively. The red regions indicate areas of high electron density with negative electrostatic potential, signifying sites favorable for electrophilic attack (proton attraction). Conversely, the blue regions correspond to areas of positive electrostatic potential, associated with electron-deficient sites that are more prone to nucleophilic repulsion due to the influence of atomic nuclei[17]. In the present study, the carbonyl oxygen atom was identified as the primary sites exhibiting negative potential (red zones), suggesting their susceptibility to electrophilic attack. The positive potential regions were primarily located around the hydroxyl groups, indicating potential sites for nucleophilic interactions. The remaining molecular regions exhibited nearly neutral potential, implying an insufficient surface charge density to participate in such reactions.

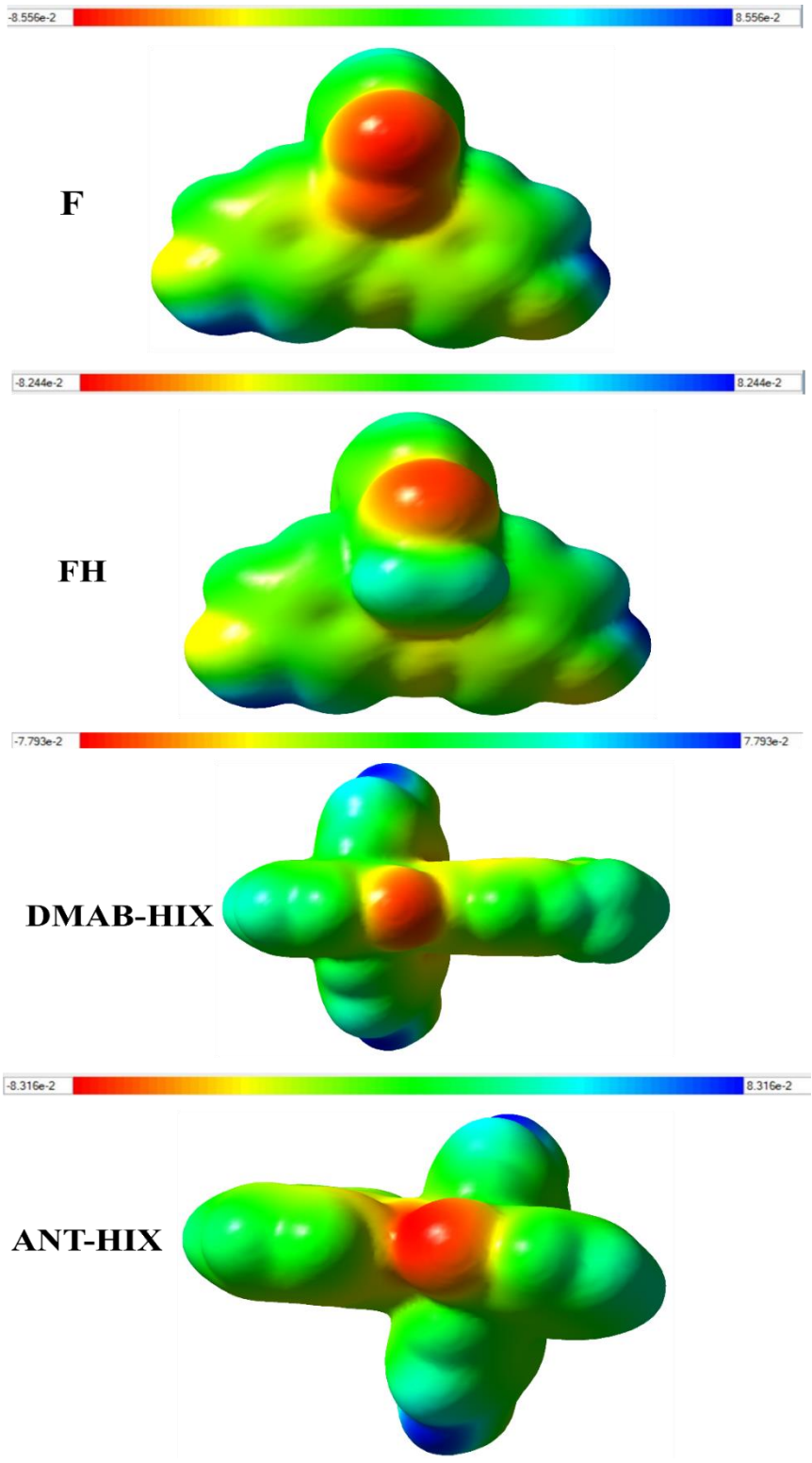

Fig. 4 MEP map for studied molecules

2.4

Chemical reactivity indices

Chemical reactivity parameters provide a reliable framework for assessing the photoelectronic properties of molecular systems. Using the energies of the HOMO and LUMO, several chemical reactivity indices were calculated for the investigated compounds. The electronic chemical potential reflects the stability of charge transfer in the ground state of a molecule. The tendency of a molecule to donate electrons is defined by the ionization potential (IP), whereas its ability to accept electrons is characterized by the electron affinity (EA). A more negative value of the chemical potential indicates grater thermodynamic stability. Molecules with a largerHOMO-LUMO energy gap are classified as hard molecules, while those with a smaller energy gap are considered soft molecules. Hard molecules are generally less reactive and less polar and exhibit higher stability than soft molecules. Chemical hardness (η) is inversely related to molecular polarizability and charge delocalization; therefore, a lower η value facilitates intramolecular charge transfer (ICT) by allowing easier redistribution of electron density within the molecule. In the case of DMAB-HIX molecule, the reduced dipole moment indicates a more symmetric charge distribution or enhanced internal charge compensation between donor and acceptor moieties. Despite this lower dipole moment, the molecule exhibits a higher chemical electrophilicity index (ω) due to its strong electron-accepting capability combined with a relatively low chemical hardness. Additionally, the high electrofugality (ΔE_e) reflects an increased tendency of DMAB-HIX to stabilize positive charge upon electron donation, which arise from effective π-conjugation and charge delocalization across the molecular framework[18].

Table 1 Chemical reactivity descriptors for studied molecules

Theoretical parameters	Descriptors	F	FH	DMAB-HIX	ANT-HIX
Total energy	-	-1145.5084 a.u.	-1180.9679 a.u.	-1584.1041 a.u.	-1757.4026 a.u.
Band gap energy (E_g)	($E_{LUMO} - E_{HOMO}$)	4.7397 eV	4.8703 eV	3.5764 eV	3.0694 eV
Ionization potential (IP)	$-E_{HOMO}$	6.0355 eV	5.8371 eV	4.7914 eV	4.9974 eV
Electron affinity (EA)	$-E_{LUMO}$	1.2958 eV	0.9668 eV	1.2149 eV	1.9280 eV
Dipole moment	-	5.1445 Debye	2.9494 Debye	0.7859 Debye	2.6956 Debye
Chemical potential(μ)	$(IP + EA)/2$	-3.6657 eV	-3.4020 eV	-3.0032 eV	-3.4627 eV
Electronegativity (χ)	-μ	3.6657 eV	3.4020 eV	3.0032 eV	3.4627 eV
Chemical hardness(η)	$E_{LUMO} - E_{HOMO}/2$	2.3699 eV	2.4352 eV	1.7882 eV	1.5347 eV
Chemical softness(s)	$1/2\eta$	0.2110 eV^{-1}	0.2053 eV^{-1}	0.2796 eV^{-1}	0.3258 eV^{-1}
Chemical electrophilicity	$\mu^2/2\eta$	2.8350 eV	2.3763 eV	4.5090 eV	3.9064 eV

index (ω)					
Electron charge transfer(ΔN_{max})	$-(\mu/\eta)$	-1.5468 eV	-1.3970 eV	-1.6795 eV	-2.2563 eV
Softness (б)	$1/\eta$	0.4220 eV^{-1}	0.4106 eV^{-1}	0.5592 eV^{-1}	0.6516 eV^{-1}
Back donation ($\Delta E_{back-donation}$)	$-\eta/4$	-0.5925 eV	-0.6088 eV	-0.4471 eV	-0.3837 eV
Nucleofugality (ΔE_n)	EA+ ω	4.1308 eV	3.3431 eV	5.7239 eV	5.8344 eV
Electrofugality (ΔE_e)	IP+ ω	8.8705 eV	8.2134 eV	9.3004 eV	8.9038 eV

2.5

Frontier molecular Orbitals

The analysis of Frontier molecular Orbitals (FMOs) provides valuable insights into the UV-Vis examination, kinetic stability, chemical bonding, optical behaviour of conjugated systems, as these properties are governed by electronic transition between the HOMO to LUMO level[19]. The distribution of charge across the HOMO to LUMO, as well as the energy difference between them, are key parameters for understanding and optimizing the optoelectronic performance of the studied molecules. The results from the FMOs analysis revealed the specific molecular regions functioning as electron donor and acceptors, demonstrating thatthese orbital features promote intramolecular charge transfer (ICT) by facilitating electron migration from donor to acceptor moieties. In this context, the HOMO primarily represents the donor orbital, whereas the LUMO serves as the acceptor orbital.

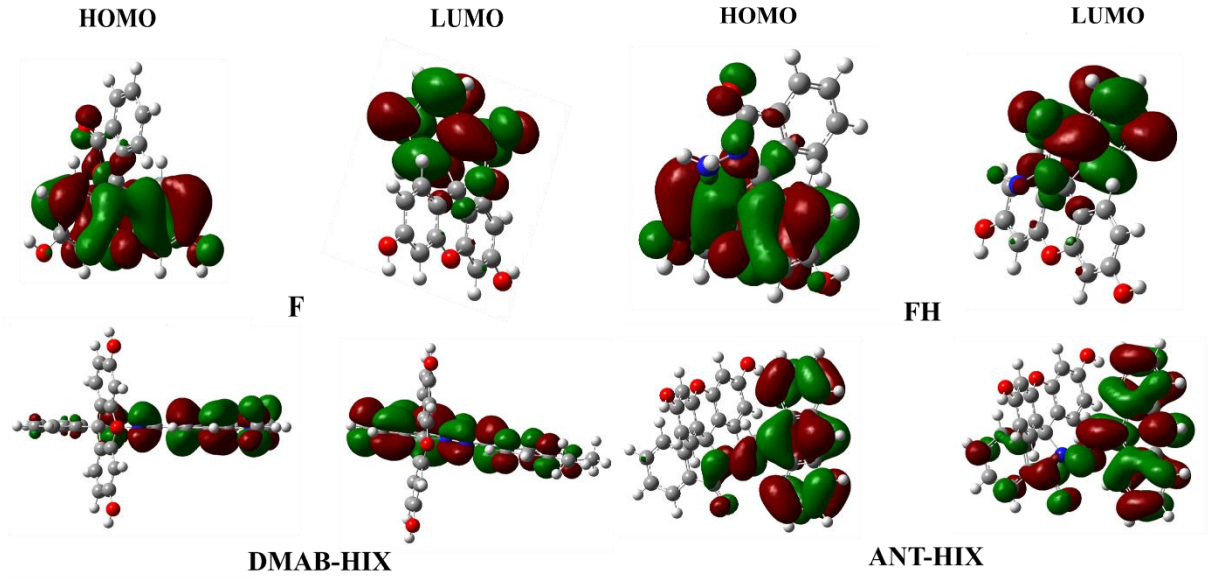

Fig. 5 Contour plots of frontier orbitals of studied molecules

For the F and FH molecules, the electron density in the HOMO was mainly occupied over the xanthene moiety, which acts as the electron-donating unit. In contrast, the electron density in the LUMO was predominantly localized on the spirolactam-linked benzene ring, identified as the electron-accepting region.Upon photoexcitation, an electron transitions from the HOMO on the xanthene core to the LUMO located on the spirolactam-fused benzene ring, signifying a clear charge-transfer process upon light absorption. For the DMAB-HIX and ANT-HIX derivatives, FMO analysis indicated that the HOMO electron density was chiefly localized over the electron-donating unit,N,N-dimethyl aminobenzene and anthracene moieties. Conversely, the LUMO electron density was concentrated on the spirolactam-fused benzene ring with strong electronic involvement from the five-membered lactam ring fused with benzene ring in DMAB-HIX and weaker participation of the five-membered lactam ring connected to the imine group in ANT-HIX. Fig. 5illustrates the spatial distribution of the HOMO and LUMO orbitals for each compound. These observations confirm that the electronic transition in all molecules occurs from the donor-rich HOMO regions to the acceptor-centered LUMO regions, which supports efficient charge transfer within the molecular framework.Otherwise, a density of states (DOS) analysis was carried out to obtain qualitative insight into the contributions of individual molecular fragments to the charge-transfer process. The DOS profiles were calculated using the GaussSum software and are presented in Fig. 6. The results clearly illustrate the influence of energetic disorder on electron and hole transport, indicating that charge transport remains relatively stable when it is governed by the principal features of the DOS distribution.

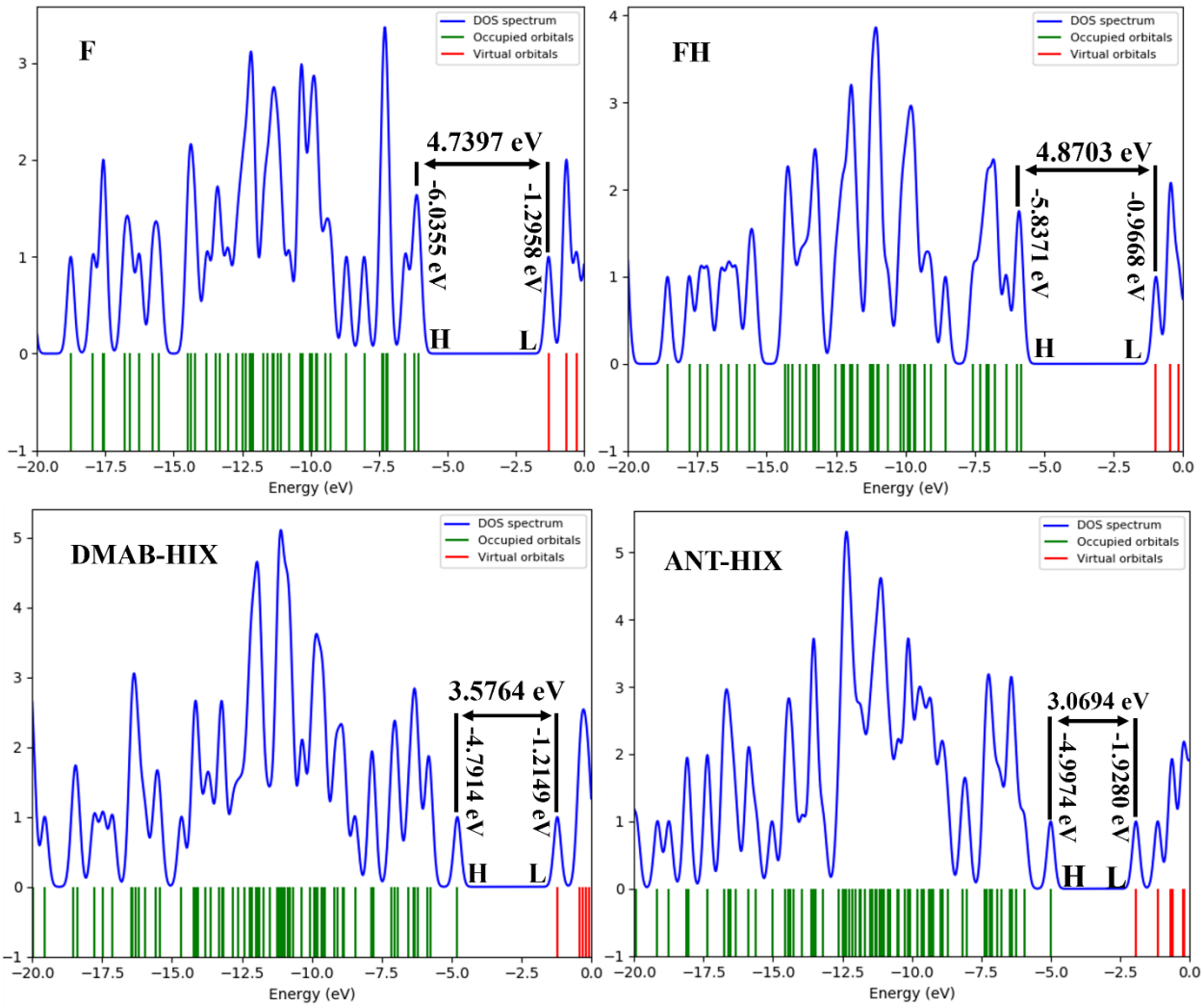

Fig. 6 Density of the state for studied molecules

2.6

Exciton binding energy (E_b)

To gain deeper insight into the optoelectronic properties of organic emissive materials used in OLEDs devices, the exciton binding energy was calculated. This parameter plays a crucial role in determining the electroluminescence quantum efficiency of organic layer in OLEDs. Exciton binding energy serves as a quantitative measure of the Columbic interaction between forces between h (hole) and e (electron). In OLED operation, injected electrons and holes recombine through Coulomb attraction within the active organic layer to form excitons, which subsequently relax radiatively, resulting in light emission[20]. A lower$E_b$indicates weaker Coulombic attraction between the hole and electron, facilitating easier exciton dissociation in the excited state. Such

behavior enhances charge separation and improves radiative recombination efficiency. The exciton binding energy can be estimated using the following equation:

$$E_b = E_{H\text{-}L} - E_{opt}$$

where, $E_{H\text{-}L}$represents the HOMO-LUMO energy gap in the ground state and E_{opt}denotes first excited energy. Using this expression, the $E_b$energiesof all functionalized xanthene-based molecule were calculated and the results are summarized in Table 2. The exciton binding energy follows the order: F < FH < DMAB-HIX < ANT-HIX, indicating that ANT-HIX possesses the highest exciton binding energy. This suggests a stronger Coulombic interaction and a higher density of charge carriers, which promotes efficient charge separation into free carriers. Consequently, ANT-HIX exhibits superior charge dissociation efficiency compared to the other studied molecules.

Table 2 HOMO/LUMO energy gap, first singlet excitation energy and exciton binding energy of studied molecules at B3LYP/6-31G(d,p).

Compound	$E_{H\text{-}L}$ (eV)	E_{opt}(eV)	$-E_b$ (eV)
F	4.7397	4.2253	0.5144
FH	4.8703	4.3662	0.5041
DMAB-HIX	3.5764	3.1079	0.4685
ANT-HIX	3.0694	2.7457	0.3237

2.7

Absorption properties

The UV-Vis absorption spectroscopy is a powerful and widely used technique for probing the ground and excited state optical properties of the molecular systems. In this studies, the ground and excited-state electronic properties of the studied molecules were investigated using a computational approach. To enhance the reliability and accuracy of the calculated absorption parameters, five density functional theory (DFT) functionals such as BPV86, B3LYP, CAM-B3LYP, B3PW91 and MPW1PW91 were employed to examine the absorption characteristic of moleculesusing time-dependent DFT (TD-DFT) in the ethanol solvent environment[21]. As shown in Fig. 7, the absorption spectrum calculated using the B3LYP functional exhibits the best agreement with previously reported experimental data. Consequently, the DFT/B3LYP method combined with the 6-31G(d,p) basis set was selected for subsequent calculations of electronic and optical properties[22].

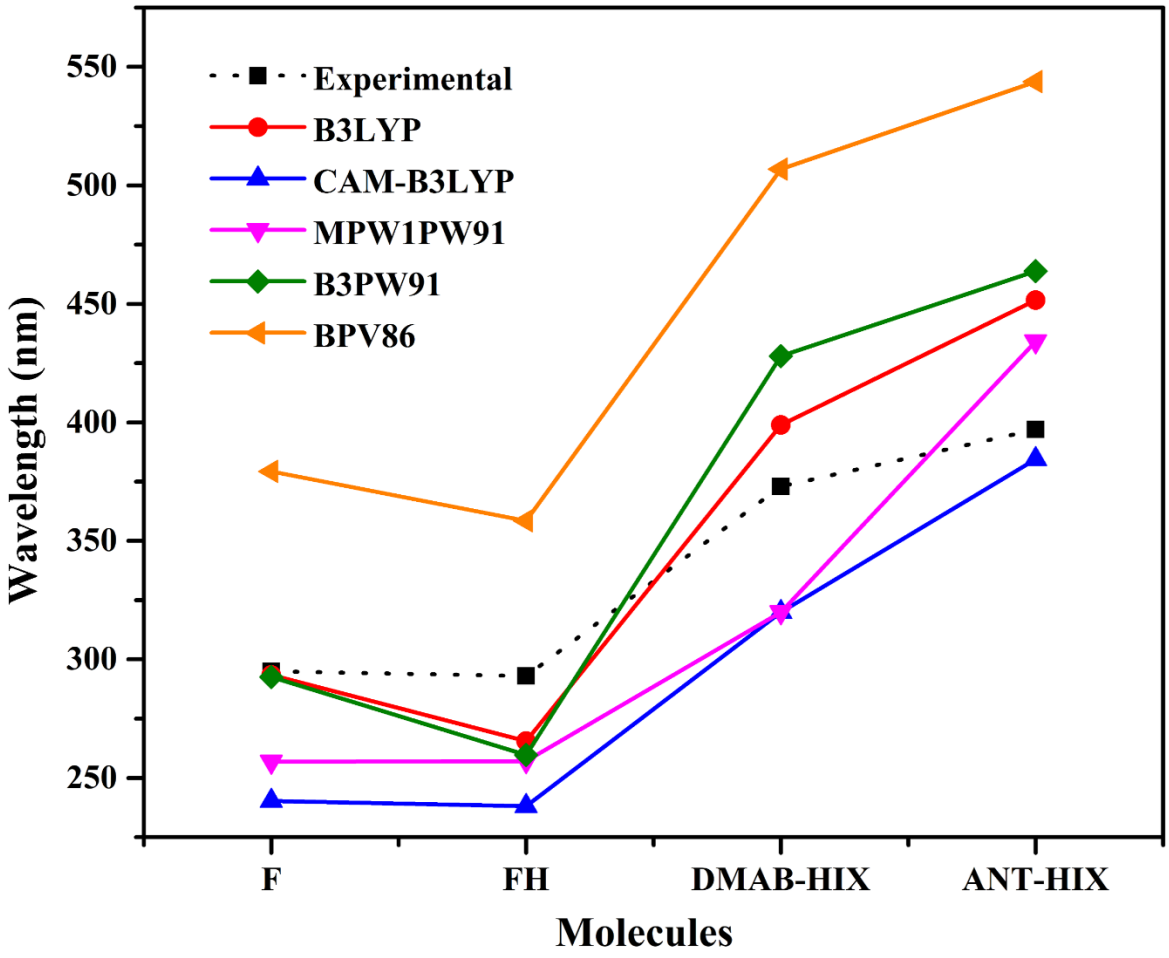

Fig. 7 Simulate λ_{max} values of studied molecules at various levels of theory in comparison with the experimental values

Fig. 8 illustrate the primary absorption peak for each molecule at its respective maximum wavelength. The transition parameters including, oscillation strength, excitation energy, absorption wavelength and major contribution of the molecular orbitals, are essential indicators of the light-harvesting efficiency of emissive materials. Among the investigated molecules, ANT-HIX exhibits the longest-wavelength absorption maximum at 451.56 nm and red-shifted absorption indicates enhanced π-conjugation and stronger intramolecular charge transfer, resulting in the lower excitation energy. The order of maximum absorption wavelengths is as follows: FH (283.96 nm) < F (293.43 nm) < DMAB-HIX (398.93 nm) < ANT-HIX (451.56 nm). For DMAB-HIX and ANT-HIX, the dominant absorption band arises from the $S_0 \rightarrow S_1$ electronic transition, which is primarily attributed to HOMO-

LUMO excitation. The higher oscillator strength and dominant HOMO-LUMO transitions suggest improved light-harvesting capability, making DMAB-HIX and ANT-HIX promising candidates for OLED application. Table 3 summarizes the simulated optical properties of the molecules, including the maximum absorptionwavelength, oscillation strength, electron transition energy and the major molecular orbitalcontribution.

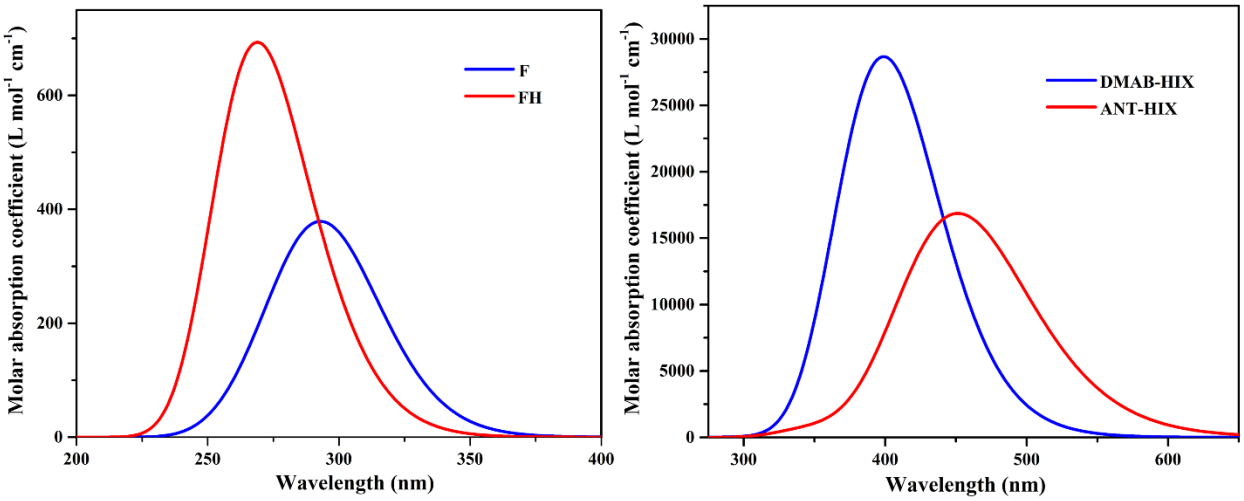

Fig. 8 Simulated absorption spectra of the studied molecules

Table 3 Computed absorption maxima, excitation energies, oscillator strength, light harvesting efficiency and the contribution of the most probable transition of the studied compounds in ethanol solvent using TD-DFT/B3LYP/6-31G(d,p) level of theory.

Molecules	Electronic transition	λ_{max} nm	Transition energy eV	Oscillator strength f_o	LHE	Assignment
F	$S_0 \rightarrow S_1$	293.43	4.2253	0.0075	0.01771	H-1 → L (98%)
FH	$S_0 \rightarrow S_1$	283.96	4.3662	0.0039	0.0089	H-1 → L (97%)
DMAB-HIX	$S_0 \rightarrow S_1$	398.93	3.1079	0.7078	0.8040	H → L (99%)
ANT-HIX	$S_0 \rightarrow S_1$	451.56	2.7457	0.4158	0.6161	H → L (99%)

2.8

Emission properties

From the result of the absorption analysis, the photoluminescence emission properties were investigated exclusively for the DMAB-HIX and ANT-HIX molecules, as these systems exhibit significant higher absorption maxima than the F and FH molecules. The emission spectra of DMAB-HIX and ANT-HIX, simulated using the TD-DFT/B3LYP method with the 6-31G(d,p) basis set are presented in Fig. 9. The maximum emission wavelengths observed at 502.02 nm for DMAB-HIX and 516.80 nm for ANT-HIX, which correspond to the radiative relaxation of electrons from the LUMO orbital to the HOMO orbital. ThecalculatedStokes shifts are 103.09 nm for DMAB-HIX and 65.24 nm for ANT-HIX, indicating substantial structural relaxation in the excited state prior to emission. Large Stokes shifts reduce self-absorption losses and impro color purity in OLED devices. In both cases, the emission wavelengths are red-shifted relative to the corresponding absorption maxima, confirming that fluorescence emission represents the reverse process of electronic absorption.Table4 summarizes the simulated optical properties of the molecules, including the maximum absorptionwavelength, oscillation strength, electron transition energy and the major molecular orbitalcontribution. A molecule with more intense florescence spectra exhibits more effective as a fluorescent OLED material.In optoelectronic devices, particularly OLEDs, shorter excited-state life times are desirable, as they promote higher radiative recombination efficiency and improved light-emission performance[23].

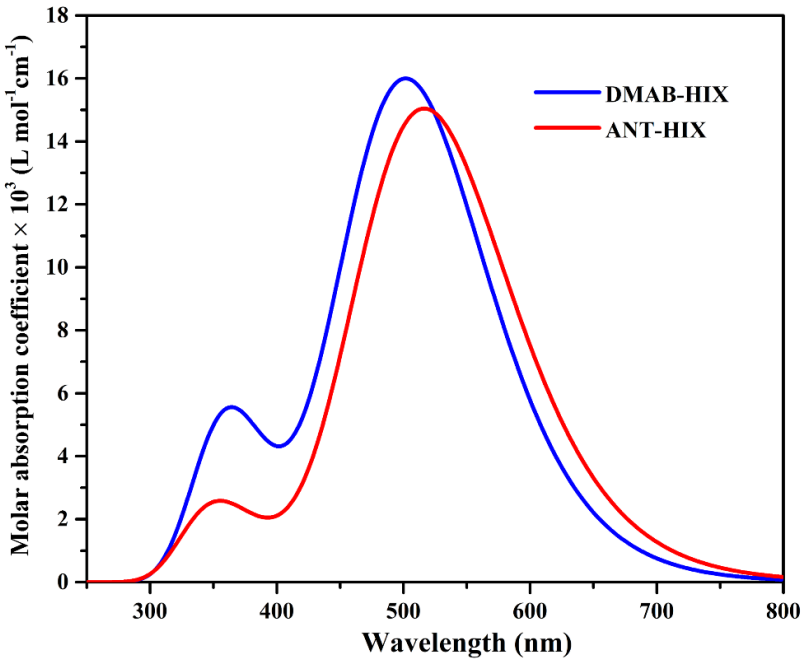

Fig. 9 Simulated emission spectraof DMAB-HIX and ANT-HIX

Table 4 Computed emission maxima, excitation energies, oscillator strength, excited state life time and the contribution of the most probable transition of the studied compounds in ethanol solvent using TD-DFT/B3LYP/6-31G(d,p) level of theory.

Molecules	Electronic transition	λ_{max} nm	Transition energy eV	Oscillator strength f_o	τ (ns)	Assignment
DMAB-HIX	$S_1 \rightarrow S_0$	502.02	2.4697	0.3945	5.34	H ← L (99%)
ANT-HIX	$S_1 \rightarrow S_0$	516.80	2.3990	0.3706	8.74	H ← L (100%)

2.9

Excited-state lifetime

The excited-state lifetime can be estimated using the following expression:

$$\tau = {}^{1.499}/_{f_0 E^2}$$

where E is the excitation energy expressed in cm^{-1} and f_0 represents the oscillator strength of the electronic excited state. Using this relation, the excited-state lifetimes of the DMAB-HIX and ANT-HIX molecules were calculated and are reported in Table 3. The results indicate that DMAB-HIX exhibits a shorter excited-state lifetime (5.34 ns) compared ANT-HIX (8.74 ns), suggesting more efficient radiative decay and reduces non-radiative decay losses, leading to improved light-emission efficiency. This shorter lifetime implies that DMAB-HIX is a more effective photon emitter, making it particularly suitable for light-emitting applications.

2.10 Light harvesting efficiency (LHE)

The light-harvesting efficiency (LHE) was evaluated using the oscillator strength obtained from TD-DFT calculations[24]. The oscillation strength corresponding to the maximum absorption wavelength provides a direst measure of the LHE. The LHE can be calculated using the following equation:

$$LHE\ (\lambda) = 1\text{-}10^{-f}$$

Where, f is the oscillator strength of the organic molecule at a given wavelength. According to this expression, larger oscillator strength values result in higher light-harvesting efficiency. The molecule with a smaller HOMO-LUMO energy gap, DMAB-HIX exhibits a higher LHE value (0.8040) compared to ANT-HIX. This enhancement indicates that the incorporation of the dimethylamino (DMA) substituent effectively improves the light-harvesting capability of DMAB-HIX through enhanced electronic delocalization and intramolecular charge transfer.

3. Conclusion

In this study, density functional theory (DFT) and time-dependent DFT (TD-DFT) calculations were employed to investigate the structural, electronic, optical

and photophysical properties of functionalized xanthene-based molecules (F, FH, DMAB-HIX and ANT-HIX) for potential optoelectronic applications. The results show that molecular functionalization significantly influences optoelectronic behaviour, excitation energies and enhanced intramolecular charge transfer. While ANT-HIX demonstrates superior charge dissociation capability, DMAB-HIX achieves an optimal balance between exciton dissociation and radiative recombination, along with shorter excited-state lifetime and higher charge-transfer characteristics induced by the dimethylamino (DMA) substituent, DMAB-HIX emerges as a promising emissive material for high-performance OLED device.

4. Reference

(1) Review, T. Chem Soc Rev. **2013**, 4963–4976. https://doi.org/10.1039/c3cs35440g.

(2) Chem, J. M.; Park, H.; Lee, J.; Kang, I.; Chu, Y.; Lee, J.; Kwon, S.; Kim, Y. Highly Rigid and Twisted Anthracene Derivatives : A Strategy for Deep Blue OLED Materials with Theoretical Limit Efficiency. **2012**, No. Table 1, 2695–2700. https://doi.org/10.1039/c2jm16056k.

(3) Nimith, K. M.; Satyanarayan, M. N.; Umesh, G. Enhancement in Fl Uorescence Quantum Yield of MEH-PPV : BT Blends for Polymer Light Emitting Diode Applications. *Opt. Mater. (Amst).***2018**, *80* (November 2017), 143–148. https://doi.org/10.1016/j.optmat.2018.04.046.

(4) Azrain, M. M.; Mansor, M. R.; Omar, G.; Fadzullah, S. H. S. M.; Esa, S. R.; Lim, L. M.; Sivakumar, D.; Nordin, M. N. A. E Ff Ect of High Thermal Stress on the Organic Light Emitting Diodes (OLEDs) Performances. *Synth. Met.***2019**, *247* (June 2018), 191–201. https://doi.org/10.1016/j.synthmet.2018.12.008.

(5) Trenor, S. R.; Shultz, A. R.; Love, B. J.; Long, T. E. Coumarins in Polymers : From Light Harvesting to Photo-Cross-Linkable Tissue Scaffolds. **2004**, No. 540.

(6) You, A.; Be, M.; In, I. Electroluminescence in Organic Crystals □. **1968**, *2043* (April 1963), 2042–2043.

(7) Wong, M. Y.; Zysman-colman, E. Purely Organic Thermally Activated Delayed Fluorescence Materials for Organic Light-Emitting Diodes. **2017**, *1605444*. https://doi.org/10.1002/adma.201605444.

(8) Findlay, N. J.; Breig, B.; Forbes, C.; Inigo, A. R.; Kanibolotsky, A. L.; Skabara, P. J. High Brightness Solution-Processed OLEDs Employing Linear, Small Molecule Emitters. **2016**, 3774–3780. https://doi.org/10.1039/c5tc03579a.

(9) Ben, N.; Elleuch, S.; Khemakhem, S.; Abid, Y.; Ammar, H. Synthesis and

Spectral Properties of Coumarins Derivatives Fl Uorescence Emitters : Experiment and DFT / TDDFT Calculations. *Opt. Mater. (Amst).***2018**, *83* (January), 138–144. https://doi.org/10.1016/j.optmat.2018.05.082.

(10) Rybakiewicz, R.; Zagorska, M.; Pron, A. Triphenylamine-Based Electroactive Compounds : Synthesis , Properties and Application to Organic Electronics Charge Transfer. *Chem. Pap.***2017**, *71* (2), 243–268. https://doi.org/10.1007/s11696-016-0097-0.

(11) Mandal, S.; Rao, G. Journal of Photochemistry & Photobiology , A : Chemistry A Computational Finding on the Effect of π -Conjugated Acceptors in Thiophene-Linked Coumarin Dyes for Potential Suitability in DSSC Application. *J. Photochem. Photobiol. A Chem.***2023**, *435* (September 2022), 114300. https://doi.org/10.1016/j.jphotochem.2022.114300.

(12) Gudeika, D.; Bezvikonnyi, O.; Masimukku, N.; Volyniuk, D.; Grazulevicius, J. V. Dyes and Pigments Tetraphenyl Ornamented Carbazolyl Disubstituted Diphenyl Sulfone as Bipolar TADF Host for Highly Efficient OLEDs with Low Efficiency Roll-Offs. *Dye. Pigment.***2021**, *194* (June), 109573. https://doi.org/10.1016/j.dyepig.2021.109573.

(13) Chen, W.; Zhu, Z.; Lee, C. Organic Light-Emitting Diodes Based on Imidazole Semiconductors. **2018**, *1800258*, 1–43. https://doi.org/10.1002/adom.201800258.

(14) Vijayalakshmi, S.; Kalyanaraman, S. Optik DFT and TD-DFT Approach for the Analysis of NLO and OLED Applications of 9-Anthraldehyde. *Opt. - Int. J. Light Electron Opt.***2014**, *125* (10), 2429–2432. https://doi.org/10.1016/j.ijleo.2013.10.104.

(15) Raftani, M.; Abram, T.; Loued, W.; Kacimi, R.; Azaid, A.; Alimi, K.; Bennani, M. N. The Optoelectronic Properties of π -Conjugated Organic Molecules Based on Terphenyl and Pyrrole for BHJ Solar Cells : DFT / TD-DFT Theoretical Study. **2021**, *10*, 489–502. https://doi.org/10.5267/j.ccl.2021.4.002.

(16) Hachi, M.; Slimi, A.; Fitri, A.; Elkhattabi, S.; Touimi, A.; Benzakour, M.; Mcharfi, M. New Small Organic Molecules Based on Thieno [2 , 3- b] Indole for Efficient Bulk Heterojunction Organic Solar Cells : A Computational Study. **2019**, *8976*. https://doi.org/10.1080/00268976.2019.1662956.

(17) Waqas, A.; Bibi, S.; Afzal, S. Substitutional Effect of Different Bridging Groups on Optical and Charge Transfer Properties of Small Bipolar Molecules for OLEDs. **2019**,

No. May, 1–12. https://doi.org/10.1002/poc.4000.

(18) Parr, R. G.; Donnelly, R. A.; Levy, M.; Palke, W. E. Electronegativity: The Density Functional Viewpoint. **1984**, *3807* (December 1981), 3801–3807.

(19) Luo, D.; Jin, R. Theoretical Characterisation and Design of D – π – A Star-Shaped Molecules with Triphenylamine as Core and Diketopyrrolopyrroles as Arms for Organic Solar Cells. **2019**, *8976*. https://doi.org/10.1080/00268976.2018.1549337.

(20) Jagadeesan, R.; Velmurugan, G.; Venuvanalingam, P. RSC Advances Better Optoelectronic Applications and Their. **2016**, *44569*, 44569–44577. https://doi.org/10.1039/c6ra04844g.

(21) Jaccob, M. The Role of p -Linkers in Tuning the Optoelectronic Properties of Triphenylamine Derivatives for Solar. **2017**, 6153–6163. https://doi.org/10.1039/c6cp07768d.

(22) Sivakumar, G.; Sasikumar, M.; Jayathirtha, V. Synthesis and Characterization of Diketopyrrolopyrrole-Based D- π -A- π -D Small Molecules for Organic Solar Cell Applications. **2017**, No. May. https://doi.org/10.1002/jhet.2795.

(23) El, I.; Zakaria, M.; Malki, E. L.; Bouachrine, M. Theoretical Investigation of Electro - Optical Properties of Novel D - Pi - D Based Organic Compounds for OLED Applications. *Opt. Quantum Electron.***2025**, *57* (3), 1–15. https://doi.org/10.1007/s11082-025-08086-3.

(24) Li, M.; Kou, L.; Diao, L.; Zhang, Q.; Li, Z.; Wu, Q.; Lu, W.; Pan, D. Theoretical Study of WS-9-Based Organic Sensitizers for Unusual Vis / NIR Absorption and Highly E Ffi Cient Dye-Sensitized Solar Cells. **2015**. https://doi.org/10.1021/acs.jpcc.5b03667.